Rheological fingerprinting of gastropod pedal mucus and synthetic complex fluids for biomimicking adhesive locomotion

Randy H. Ewoldt,[a] Christian Clasen,[b] A. E. Hosoi [a] and Gareth H. McKinley*[a]

[a] *MIT, Department of Mechanical Engineering, Hatsopoulos Microfluids Laboratory, Cambridge, MA, 02139 USA. E-mail: gareth@mit.edu*

[b] *Departement Chemische Ingenieurstechnieken, Katholieke Universiteit Leuven, W. de Croylaan 46, 3001 Heverlee, Belgium*

† Electronic Supplementary Information (ESI) available: See http://dx.doi.org/10.1039/b000000x/

Nonlinear rheological properties are often relevant in understanding the response of a material to its intended environment. For example many gastropods crawl on a thin layer of pedal mucus using a technique called adhesive locomotion, in which the gel structure is periodically ruptured and reformed. We present a mechanical model that captures the key features of this process and which suggests that the most important properties for optimal inclined locomotion are a large, reversible yield stress, followed by a small shear viscosity and a short thixotropic restructuring time. We present detailed rheological measurements of native pedal mucus in both the linear and nonlinear viscoelastic regimes and compare this "rheological fingerprint" with corresponding observations of two bioinspired slime simulants, a polymer gel and a clay-based colloidal gel, that are selected on the basis of their macroscopic rheological similarities to gastropod mucin gels. Adhesive locomotion (of snails or mechanical crawlers) imposes large amplitude pulsatile simple shear flow onto the supporting complex fluid, motivating the characterization of nonlinear rheological properties with large amplitude oscillatory shear (LAOS). We represent our results in the form of Lissajous curves of oscillatory stress against time varying strain. The native pedal mucus gel is found to exhibit a pronounced strain-stiffening response, which is not imitated by either simulant.

1. Introduction

Many gastropods, such as snails and slugs, crawl using a technique called adhesive locomotion, in which a thin layer (typically 10-20 μm) of excreted mucus serves both as glue and lubricant[1, 2], allowing the animals to climb walls and crawl across ceilings. These gastropods exert shear stresses on this thin layer of structurally-sensitive mucus that holds the organism to the substrate. The pedal mucus has an effective yield stress; at high applied stresses the network structure breaks, enabling the foot to glide forward over a fluid layer; whereas in regions of low applied stress the network structure reforms into a solid-like layer connecting the foot to the substrate (Figure 1). Gastropod pedal mucus films are physically crosslinked gels containing 0.3-9.9% (by weight) solid matter in water.[3] The solid constituent which dominates the mechanical properties is a mucus protein-polysaccharide complex. The glycoconjugates present in pedal mucus share similarities with both mucin glycoproteins and glycosaminoglycans in vertebrates.[3]

A mechanical crawler has recently been constructed which crawls using the principle of adhesive locomotion.[4] The success of the mechanical crawler depends critically on both the mechanical design of the robot and the rheological properties of the slime simulant. Here we compare the rheological properties of natural pedal mucus from terrestrial gastropods with two bioinspired slime simulants that have been employed as adhesives by the mechanical crawler. The first is a polymeric gel based on Carbopol 940 and the second is a colloidal gel based on the synthetic clay LaponiteRD. Carbopols are a family of high molecular weight polymers consisting of cross-linked poly(acrylic acid) differing in crosslink density and degree of branching,[5] which are used to modify the rheology of a variety of personal care products. Carbopol dispersions are typically interpreted as microgels[5, 6], in which soft crosslinked polymer particles are formed and swell in water. The outside of each particle exposes dangling ends which overlap with the dangling ends of other particles above a critical concentration, producing a sample-spanning network structure.

LaponiteRD is a disc-shaped colloidal particle measuring approximately 300 Å in diameter and 10 Å in thickness.[7] Laponite clay particles form a fractal network when mixed with water at sufficient concentration.[8] If the colloidal dispersion is properly filtered, however, it forms a colloidal glass.[9]

We use a series of linear and nonlinear rheological tests to construct a "fingerprint" of the materials. With steady-state flow viscosity tests we show that both slime simulants satisfy a minimum yield stress criteria needed for wall climbing. In addition, we demonstrate that the linear viscoelastic behavior at low strain amplitudes of both simulants is similar to native slime. However, adhesive locomotion imposes large stresses and strains upon the material, and thus the nonlinear rheological response of slime is relevant to the dynamics of adhesive crawling. The relevant conditions for characterizing the mucin gel and simulants is large amplitude oscillatory shear (LAOS), and our measurements show that the mechanical response leading up to yield is different for the simulants compared to native slug slime; the native slime exhibits pronounced strain-stiffening as observed with Lissajous curves, and neither simulant mimics this. Other recent rheological studies have shown that similar strain-stiffening responses are ubiquitous in biopolymer gels.[10]

2. Experimental

Pedal mucus was collected from the terrestrial snail *Helix aspera* and the terrestrial slug *Limax maximus*, which were kept in glass terrariums and supplied with a diet of green leaf lettuce and occasionally carrots. A single animal was removed from the containment area, placed on a glass plate, and allowed to crawl toward a piece of food. No mucus was collected until the gastropod had travelled a minimum of one body length so that no debris from the containment area remained in the sample, and to help ensure that locomotive mucus was present, rather than adhesive mucus which has been shown in some cases to have different compositional and mechanical properties.[11] The deposited trail mucus was gathered by scraping with a razor blade behind the crawling animal

until an adequate sample size was obtained. The sample was immediately deposited on the Peltier plate of a rheometer for testing.

Carbopol 940 was obtained from the Noveon corporation (Cleveland, OH). Slime simulants based on Carbopol were prepared at various concentrations ranging from 0.5% – 4% (w/w), where w/w refers to weight of the additive with respect to the total weight of the mixture. The polymer was obtained as a white powder, and was added to deionized water being agitated with a magnetic stirrer. Samples were mixed for a minimum of 30 minutes. The Carbopol-water mixtures initially have a pH near 3, and each was neutralized with 4 M NaOH solution to achieve a pH=7, producing a clear gel at the targeted concentration. The rheology of Carbopol mixtures depends on the pH, with maximum thickening occurring within a pH range of 5-9.[12]

LaponiteRD was obtained from Rockwood Specialties Group, Inc. (Princeton, NJ). Simulants based on Laponite were prepared at concentrations ranging from 1% – 7% (w/w). Dispersions were prepared by adding Laponite powder to deionized water being agitated with a magnetic stirrer. Samples were mixed for 30 minutes and degassed to remove air bubbles. In all cases a clear solution was formed. Laponite dispersions were brought to pH=10 by addition of NaOH to make them chemically stable.[13] Dispersions were kept in a sealed container and allowed to rest for a minimum of 6 hours before testing.

Rheological measurements were performed with stress-controlled AR1000-N and AR-G2 rheometers, and a strain-controlled ARES-LS rheometer (all TA Instruments, New Castle, DE). Samples were tested between both plate-plate and cone-plate geometries, at all times using a solvent trap to stifle evaporation. For plate-plate geometries, diameters ranged from 0.8 cm to 4 cm, and gaps ranged from 200 μm to 1000 μm. When necessary, adhesive-backed waterproof sandpaper (2000 grit, Eastwood Co., Pottstown, PA) was attached to the top and bottom plates to help avoid slip at the boundaries. Cone-plate geometries were used for low viscosity Laponite mixtures. Two cones were used; a 4 cm 2° cone with 57 μm truncation and a 6 cm 1° cone with 28

μm truncation. All samples were tested at T=22 °C. Immediately before testing, Laponite samples were subjected to a controlled pre-shear at a shear rate $\dot{\gamma} = 5\,\mathrm{s}^{-1}$ for 25 seconds, followed by three minutes of recovery. This pre-shear and recovery sequence helped to mitigate strain history and aging effects, as Laponite is known to be thixotropic and to exhibit rheological aging, even under quiescent conditions.[8] A carefully controlled and documented sample preparation history is thus essential in order to achieve reproducible results. It is likely that Laponite continues to slowly age after the three minutes of recovery, but this was not observed to affect the primary results of this work.

3. Results and Discussion

3.1. Requirements of Slime Simulants

A simple model is used to determine which fluid properties are desired for adhesive locomotion. The model consists of discrete pads actuated by an internal force (Figure 2), which may be interpreted as a discrete form of gastropod locomotion or a generalized model of Chan's Robosnail II.[4] The crawler rests on a layer of fluid, and a controlled internal force F separates one pad away from the rest, while the rest are rigidly connected. The controlled force might come from muscles in real gastropods or from the actuators of a mechanical crawler. This internal force acts in equal and opposite directions on the two portions that are "rearward tending" and "forward tending." It is assumed that the pads are rigid and the no-slip condition is satisfied across the surface of each pad. The actuation force balances instantaneously with the shear resistance of the fluid and the weight of the pads when inertial effects are negligible.

It can be shown that adhesive locomotion requires, at a minimum, a non-Newtonian fluid viscosity.[14] Here we consider the case of idealized inclined locomotion. If the crawler is to passively keep its place on an inclined surface, yet move forward while attempting to crawl, the fluid must exhibit a rheologically-reversible apparent yield stress. This is a specific form of the rheoreversibility discussed by Carretti et al.[15]; the material for this application must regain its

solid-like properties at low stress without the need to change environmental variables such as temperature or pH. A rheologically-reversible yield stress is characteristic of weak gels, as opposed to strong gels.[16] While strong gels are solid-like and may rupture at a critical stress, they do not flow above the rupture stress, nor do they regain their solid-like nature when the stress is removed. For example, gelatin ruptures above a critical stress, but the temperature must be cycled for the pieces to recombine into a unified solid.

Inclined adhesive locomotion requires a minimum yield stress. The minimum *static* yield stress that is required for the crawler to rest on an inclined surface is $\tau_y \geq Mg\sin\theta/A$, where A is the total contact area. The minimum yield stress required to move forward, however, is higher than the minimum static yield stress. Consider a crawler with total contact area A, consisting of N pads (Figure 2), each bearing an equal portion of the total weight Mg, traversing a surface inclined at an angle θ with the horizontal. Although we consider our model to be general, some relevant dimensions for Robosnail II are $Mg \approx 0.31\ \text{N}$, $A \approx 35\ \text{cm}^2$, $N = 5$, and overall length approximately $15\ \text{cm}$.[17] The discrete pad model can be generalized with $\phi = 1/N$, which represents the fraction of the crawler that is moving forward during actuation. If the crawler is connected to the substrate via a complex fluid having a yield stress τ_y, then to move forward a minimum actuation force must support the pad weight and exceed the yield stress, $F_{\min} = \tau_y \phi A + \phi Mg\sin\theta$. The force can not be too large, however, or the rearward-tending pads will also cause the fluid under them to yield. The maximum actuating force is then expressed as $F_{\max} = \tau_y (1-\phi) A - Mg\sin\theta(1-\phi)$. When these two forces are equal, the crawler is unable to make progress since the material under all pads would yield simultaneously. This critical point, at which $F_{\min} = F_{\max}$, can be recast in terms of a minimum dynamic yield stress which is required for locomotion, given by

$$(\tau_y)_{\min} = \frac{Mg\sin\theta}{A}\left[\frac{1}{1-2\phi}\right]. \qquad (1)$$

The minimum dynamic yield stress is therefore a factor of $1/(1-2\phi)$ larger than the static yield stress. This can be used as a design criteria when choosing a slime simulant. For example, with Robosnail II, which has five pads, the required locomotive yield stress is approximately 67% higher than the necessary static yield stress for inclined locomotion. The assumption of equipartition of weight among the pads makes Eq (1) a lower bound; a higher yield stress is required if any pad carries more than the equipartion weight. The upper bound for the required yield stress occurs when one pad happens to support the entire weight of the crawler, $\left(\tau_y\right)_{\max} = Mg\sin\theta/\phi A$. Although the simplest models of yield stress fluids assume affine yielding of the material, the model results presented above are independent of the nature of yield. For example, if the material experiences adhesive yielding (i.e. slip at the wall) the above analysis still applies provided the adhesive nature of the yield event is reversible and the pad can passively reattach at low stress.

Once the forward-tending pad has yielded the fluid, the speed of the crawler is inversely proportional to the flow viscosity. The center of mass velocity is $V_{cm} = hF/A\eta$, assuming steady viscous Couette flow above the yield point and a crawler mass equally distributed among the pads. For non-affine yielding and flow the velocity expression must be modified. However, velocity is still inversely related to the resistance to relative motion (viscosity or sliding friction). Thus, another material property to be considered for optimization is the post-yield viscosity, which should be minimized to increase the speed of the crawler.

The final property considered here is the restructuring time required for the sheared fluid to regain its yield stress. This time-dependent character of viscometric material functions in which structure breaks down during flow and builds up during rest is known as thixotropy, and is

ubiquitous in yield stress materials.[18, 19] This finite restructuring time imposes limits on the maximum velocity of an adhesive locomotion crawler. After moving a portion of its foot forward, a crawler must wait for the material to regain an adequate yield stress before actuating the next portion. Thus, the restructuring time must also be minimized to increase crawler speed. It should be noted that living gastropods may optimize pedal mucus properties with respect to an alternative cost function, since the organisms must expend significant energy to produce the mucus,[20, 21] unlike a mechanical crawler.

Figure 3 is a nomogram that represents candidate slime simulants in terms of two of the important fluid properties: yield stress and post-yield viscosity; for clarity the restructuring time is not shown in this two-dimensional projection. Post-yield viscosity values are taken at a shear rate $\dot{\gamma} = 10\ \mathrm{s}^{-1}$, which is a representative shear rate for Robosnail II, since the pad velocity is $V_i \approx 1\ \mathrm{cm.s}^{-1}$ and the fluid thickness is $h \approx 1\ \mathrm{mm}$. A line of minimum locomotive yield stress for vertical wall climbing can be drawn for Robosnail II, such that any simulant below this line will not meet the criteria for vertical wall climbing. Lines of constant Bingham number are plotted on the figure as a guide to the eye. The Bingham number is motivated by the Bingham model for a yield stress fluid[22], and is given by $Bn = \tau_y / \eta\dot{\gamma}$, where τ_y is the yield stress, η is the viscosity, and $\dot{\gamma}$ is the shear rate, again we take $\dot{\gamma} = 10\ \mathrm{s}^{-1}$ for the Bingham numbers to be consistent with the post-yield viscosity data. For the case of a vertical climber the Bingham number represents a comparative measure of support forces and resistive forces, therefore high *Bn* values are desirable; increasing the yield stress contributes (linearly) to the factor of safety of wall-climbing whilst decreasing viscous stress increases crawler speed, as noted above.

It can be seen from Figure 3 that there are slime simulants which meet the minimum rheological criteria for a wall climbing mechanical crawler that uses adhesive locomotion. Thus, although native slug slime could be used for a mechanical crawler, harvesting slime is not required to

operate a mechanical wall climbing device. Furthermore, from Eq (1) it is clear that the minimum required yield stress scales with the areal mass density, and therefore scales as the characteristic length of the crawler, $\tau_y \propto Mg/A \propto L$. Thus, for geometrically similar devices a smaller crawler will require a lower yield stress and a wider range of fluids will be appropriate for use as adhesive lubricants.

3.2. Rheological Material Functions

Two promising slime simulants, a particulate gel based on Laponite and a polymeric gel based on Carbopol, were examined in detail and compared with native pedal mucus from the terrestrial snail *Helix aspera* and the terrestrial slug *Limax maximus*.

3.2.1. Steady Shear Flow

The steady shear viscosity of the Carbopol-based and Laponite-based simulants and native pedal mucus from *Helix aspera* are shown in Figure 4. Data is shown for two different samples of pedal mucus. At sufficient concentration, each simulant exhibits a very large viscosity at low stress. For $\tau \lesssim \tau_y$ the viscosity for these materials is so high that they are solid-like for timescales on the order of seconds, which is the relevant timescale of locomotion for natural gastropods[23] and for Chan's mechanical crawler. For example, with a viscosity $\eta \approx 10^6$ Pa.s, and a fluid thickness $h = 1$ mm, Chan's crawler would slump down a vertical wall at a rate of only 0.3 mm.hr^{-1}. However, at a critical stress the viscosity decreases by several orders of magnitude. Since flow exists for any finite stress, none of these materials exhibits a true yield stress. However, this behavior may be described as an apparent yield stress, since the flow at low applied stresses may be difficult to observe, and it is followed by a dramatic drop in viscosity over a narrow range of stress. The critical stress at which the viscosity dramatically changes will henceforth be referred to as the yield stress.[24, 25]

Some flow curves appear to be slightly shear-thickening below the yield stress (e.g. native slime). This is not uncommon for yield stress fluids, because the stress is incrementally increased after the apparent steady-state flow is achieved, and a very large equilibration time exists below the yield stress.[26] Native slime and the Laponite gel share a steep and dramatic drop in viscosity at the yield stress (Figure 4b), whereas the viscosity of the Carbopol solutions drops less quickly as stress is increased (Figure 4a). The drop in viscosity of Laponite occurs over such a narrow range of stress that a stress-sweep could not capture the behavior. Thus, a rate-sweep was performed from high shear-rates down to low shear-rates. This technique enables large changes in the steady shear viscosity to be measured over a small change in stress. A stress-sweep was used to explore the high viscosity region of the flow curve, since the data was beyond the minimum resolvable range of the rate-sweep.

Each of these materials is rheologically reversible, so that solid-like properties are regained when the stress is reduced below the yield stress, and the test can be repeated to give the same data. The timescale over which the material restructures is known as the thixotropic timescale[18], which may affect the value of the measured yield stress[19]; this will be discussed further in Section 3.2.4.

The data for both simulants show that the yield stress is a strong function of concentration. The maximum yield stress of each simulant is limited by the impracticality of increasing the concentration beyond a certain point. Extremely high yield stress materials are also difficult to test, since they suffer from slip at the boundaries.[27] Wall slip can be witnessed by observing the edge of the sample during the test[28]; this method indicates that Laponite at 7% is prone to slippage at the solid boundary. Thus, the data reported in Figure 4b give the apparent viscosity for a large gap $h = 1000\ \mu\text{m}$; if slip is occurring then the measured viscosity will become a function of gap height.[29]

3.2.2. Linear Viscoelasticity

The linear viscoelasticity of the materials was examined with small amplitude oscillatory shear (SAOS). The native slime is compared here to simulants which have similar yield stress values: a Carbopol-based simulant at 2% and a Laponite-based simulant at 5%, each having a yield stress $\tau_y \approx 100$ Pa. The linear rheological regime is defined such that the material properties are not a function of the input stress amplitude, and thus each oscillation test in the linear regime is performed below the yield stress ($\tau_0 \ll \tau_y$).

The linear viscoelastic moduli, G' and G'', were examined over a range of frequencies using SAOS. Both the elastic and viscous contributions to the complex modulus were found to be weak functions of frequency for each sample below the yield stress, as shown in Figure 5. Although each material has approximately the same yield stress, the storage moduli vary by over an order of magnitude; native slime has the lowest elastic modulus, near 200 Pa, whereas the particulate gel Laponite has a storage modulus ten times larger, $G' \approx 2000$ Pa. The mesh size of a polymer gel may be estimated from the expression $G \sim kT/\xi^3$, where ξ is the characteristic length scale of the mesh,[30] resulting in $\xi \sim 30$ nm for pedal mucus and $\xi \sim 20$ nm for Carbopol.

3.2.3. Large Amplitude Oscillatory Shear (LAOS)

A crawling slug subjects the pedal mucus film to shear stresses that exceed the yield stress, and thus the large amplitude, nonlinear viscoelastic properties of both native slime and slime simulants are relevant in adhesive locomotion. The shear stress exerted by a crawling slug can exceed 2000 Pa, as measured by Denny.[23] Furthermore, the strain amplitude under a crawling slug can be estimated from the speed versus time profile reported by Denny.[23] Using this data, and assuming the pedal mucus thickness $h = 20\,\mu$m, a strain amplitude $\gamma \sim O(10^2)$ is imposed on the pedal mucus with each pulsatile wave.

The response of a material to oscillatory shear is considered nonlinear if the storage and loss moduli depend on the input stress (or strain) amplitude. Additionally, the strain (or stress) response may be observed to contain higher harmonics than the input frequency, rather than exhibiting a pure harmonic response. In this nonlinear regime the linear viscoelastic moduli G' and G'' are not uniquely defined. The complex fluid response can be analyzed with a Fourier transform[31], and the real and imaginary coefficients of the higher harmonic contributions can be represented as G_n' and G_n'' respectively (for n = 1, 2, 3, …). To be precise, we will therefore report the first harmonic elastic and loss moduli, G_1' and G_1'', for LAOS results, which reduce to G' and G'' in the limit of a small amplitude deformation history.

The first harmonic of the storage modulus G_1' and loss modulus G_1'' are shown in Figure 6 as a function of stress amplitude τ_0 at a fixed frequency of $\omega = 1$ rad.s^{-1}. At low stresses each material shows little or no dependence on the input stress amplitude. Each material undergoes a transition at a critical stress at which the elastic response dramatically decreases. However, no data could be collected for native slime beyond this critical stress since the material was ejected from the gap. The critical stress amplitude for this transition corresponds approximately to the apparent yield stress observed in steady flow tests (Figure 4). The sharpness of the transition also corresponds with the steady shear flow results; the polymer gel simulant exhibits a gentle stress softening, whereas the slime and particulate gel simulant show a very sharp transition at a critical stress.

The critical yield strain may be expected to obey the relationship $\tau_y \sim G\gamma_y$ where G is the nominal elastic modulus of the material. This is approximately true for the simulants. The yield stresses are similar and the elastic modulus of the Laponite gel is approximately three times that of the Carbopol. This difference in elastic modulus is therefore compensated by changes in the critical strain. The critical yield strain for the particulate gel Laponite is smaller (by

approximately six times) than the polymer-based Carbopol gel; the particulate-based material requires a smaller imposed strain to disrupt the equilibrium microstructure.

As the oscillatory stress amplitude approaches the yield stress, small differences can be seen in the behavior of G_1' and G_1'' for each material. The loss modulus G_1'' appears to increase just before yield for each material; this increase is most pronounced with the Carbopol simulant. The increase in G_1'' prior to yield, combined with a decrease in G_1', has been observed in other materials and is classified as type III LAOS behavior by Hyun and coworkers.[32] This type III behaviour can be qualitatively explained by considering a relaxation time that is shear-rate dependent, as is likely the case for metastable yield stress fluids; a peak in G_1'' can then be reproduced by simply modifying a Maxwell model in this way.[33] The variation of the first harmonic storage modulus is less interesting as the yield stress is approached; in each case G_1' is a weak function of stress amplitude for $\tau_0 < \tau_y$. However, upon closer inspection, a dramatic difference in the material response leading up to failure becomes apparent.

With the aid of Lissajous curves one can immediately see the substantial difference in each material's non-linear response to an oscillatory stress input $\tau(t) = \tau_0 \cos(\omega t)$, as demonstrated in Figure 7, Figure 8, and Figure 9. These Lissajous curves are parametric plots of stress versus strain, with each curve corresponding to an oscillatory shear test with a sinusoidal stress input at a particular frequency and amplitude. The trajectory is elliptic for a linear viscoelastic material, approaching the limiting case of a straight line with slope *G* for a Hookean elastic solid and an ellipse with axes aligned with the coordinate axes for a Newtonian fluid. A nonlinear material response to a harmonic forcing input will distort this ellipse. The cyclic integral of a Lissajous curve, in which stress is plotted against strain, is equal to the energy dissipated per unit volume per cycle, E_d, and is directly related to the loss modulus G_1'' as $E_d = \pi \gamma_0^2 G_1''$.[34]

The Lissajous curves for each material at low stress appear as tight ellipses (see insets in Figure 7, Figure 8, and Figure 9) indicating $G' \gg G''$; only a small area is enclosed and the response is dominated by elasticity. As the imposed stress amplitude is increased toward the yield stress each material exhibits distinctive behavior. The Laponite simulant maintains tight elliptical curves almost all the way up to yield, and subsequently undergoes a quick transition to predominantly viscous behavior, as shown by a dramatic increase in the area enclosed by the curve. This transition is consistent with the sudden drop in viscosity for the steady state flow curves (Figure 4b), and is related to the fragility of the colloidal gel microstructure. The Lissajous curves for the Carbopol (Figure 7) progressively broaden to enclose more area, and thus show a gradual transition from elastic to viscous behavior. This soft transition is consistent with the steady state flow tests (Figure 4a) and the behavior of G_1' and G_1'' as the oscillatory stress amplitude is increased (Figure 6a). To aid comparison, we use the same ranges on the abscissa and ordinate of Figure 7 and Figure 8; Figure 9 shares the same aspect ratio but with a larger range.

In contrast to the two simulants, the native pedal mucus exhibits a strongly nonlinear response leading up to yield. For native slime the elliptical curves which are present at low stresses become progressively distorted as the stress amplitude is increased. The distortion is such that the stress increases sharply at large strains. This upturn in stress can be interpreted as a form of strain-stiffening, since the maximum stress is higher than would be expected if the small strain response were fit to an ellipse and projected to large strains. It is significant to note that this nonlinear response is not captured by monitoring G_1', as shown in Figure 6, in which the first harmonic storage modulus of native slime is a very weak function of stress amplitude. The strain-stiffening reported for native slime is not mimicked by either of the Carbopol or Laponite gel simulants. Although strain-stiffening is required in other biomaterial applications (e.g. arterial walls[35]), and

may also be important in biological adhesive locomotion, our simple adhesive locomotion model is not affected by this behavior.

It is important to point out that nonlinear LAOS behaviour depends on (at least) two parameters: stress (or strain) amplitude and frequency. Here we have only explored one-dimension of this parameter space; i.e. the rheological response to increasing oscillatory stress amplitudes at a constant frequency. A framework for exploring the two-dimensional experimental space, along with quantifying the nonlinear stiffening behaviour, is the subject of ongoing work.[36]

3.2.4 Time Dependency of the Yield Stress

The apparent yield stress of a material is likely to depend on how long the sample has been at rest since it was last yielded, i.e. there is a natural timescale of restructuring (thixotropy) to regain a yield stress.[18, 19] Furthermore, our simple model shows that the maximum velocity of a mechanical crawler is inversely related to the restructuring time.[14]

The restructuring times of the Carbopol and Laponite gel simulants were examined using shear stress overshoot tests.[37] The sample is first pre-sheared to break down structure, i.e. it is "shear rejuvenated"[38], to yield the material and erase any strain history effects. The pre-shear is abruptly "quenched," or brought to a halt, at which point the sample is allowed to age for a waiting time t_w. A step-strain-rate is then imposed, which destroys the existing microstructure and causes the sample to flow. The resulting overshoot stress $\Delta\tau$ is then determined as the difference between the peak shear stress and the steady flow stress, and is expected to depend on the time t_w that the microstructure has been allowed to equilibrate. The overshoot stress is not quantitatively equivalent to the yield stress as defined in this work. However, it is closely correlated to the yield stress, as it is the peak stress which occurs as the strain is increased and the material microstructure is ruptured.

The results of time-dependent overshoot tests for the simulants are shown in Figure 10. The Laponite sample (3%) was pre-sheared at $\dot{\gamma} = 5\ \text{s}^{-1}$ for 60 seconds. Less shearing was needed to eliminate strain history effects with the Carbopol, which was pre-sheared at $\dot{\gamma} = 5\ \text{s}^{-1}$ for five seconds. Each was allowed to rest for a specified time and then sheared once more at $\dot{\gamma} = 5\ \text{s}^{-1}$. Each Carbopol test was repeated three times and error bars are shown. The minimum waiting time allowed by the rheometer is one second, which provides a lower bound for measurement of thixotropic recovery.

An appropriate form of the rheological aging observed in the samples is a stretched exponential approach to an asymptotic value observed at long rest times

$$\Delta\tau\left(t_w, \dot{\gamma}\right) = \Delta\tau_\infty\left(\dot{\gamma}\right)\left(1 - e^{-\left(t_w/\lambda\right)^B}\right) \qquad (2)$$

where $\Delta\tau_\infty$ is the maximum overshoot stress at long rest times, t_w is the rest time, λ is the characteristic restructuring time, and B is the stretching exponent. Stretched exponentials have been observed experimentally in both polymeric[39] and colloidal[40] systems and have been associated with the presence of fractal networks.[41] When $B = 1$, Equation (2) represents a single exponential aging timescale, which has previously been used to describe the aging of the yield stress.[42] Each data set in Figure 10 has been fitted to Eq (2) as both a single exponential ($B = 1$) and a stretched exponential. The regression results are shown in Figure 10.

For a yield stress that grows in a similar fashion to Equation (2), the restructuring time λ is inversely related to the maximum velocity of a mechanical crawler.[14] The polymer gel has a much faster restructuring time than the particulate gel. The single exponential restructuring timescale of Carbopol is $\lambda \approx 0.8\ \text{s}$, whereas the restructuring time of Laponite dispersions is $\lambda \approx 17\ \text{s}$. Thus, the maximum velocity of a mechanical crawler on Carbopol would (theoretically) be

approximately 20 times that of a crawler on Laponite. The stretched exponential timescales are also dramatically different.

The restructuring timescale of native pedal mucus could not be reliably measured as a result of technical difficulties. However, Denny performed similar overshoot tests with gastropod pedal mucus and found that peak stress as a function of wait time could be fit to a power law.[43] In order to extract a timescale of restructuring for comparison, a single exponential timescale can be fit to the first ten seconds of this power law giving $\lambda \approx 0.85$ s with R^2=0.74. Although there is biological variability and a low R^2 value, it is apparent that pedal mucus and the Carbopol gel share restructuring times of the same order of magnitude.

4. Conclusions

It has been known for some time that pedal mucus from terrestrial gastropods exhibits a yield stress,[2] but the present work is the first examination of the progressive transition from an elastic gelled solid to a nonlinear viscoelastic fluid as the oscillatory shear stress amplitude is increased. Lissajous curves (such as Figure 9) can be used to graphically indicate the observed strain-stiffening behavior of native pedal mucus. The bulk rheological response of native slime was used to provide a set of benchmarks for comparing two possible complex fluids (a particulate gel and a polymeric gel) for the purpose of enabling mechanical adhesive locomotion.

A large number of structured materials were surveyed as possible slime simulants, including polymer gels, particulate gels, emulsions, wet foams, and composites (Figure 3). Two simulants which could be formulated to have similar yield stresses to that of native slime (Figure 4) were then chosen for further study. When examined in detail, in linear and nonlinear deformation, the simulants show some differences in rheological properties.

Table 1 summarizes the results of the comparison of these simulants with native gastropod pedal mucus.

The three key parameters for a complex fluid to be useful in adhesive locomotion are a high yield stress, τ_y, to support the crawler on an inclined surface, a low post yield viscosity, η, to increase speed, and a small restructuring timescale, λ, also to increase speed. Of the two simulants analyzed in this work, the Carbopol-based polymer gel is the best candidate for use in adhesive locomotion. It provides sufficient yield stress, a moderate post-yield viscosity, and a restructuring time that is more than an order of magnitude smaller than the Laponite-based colloidal gel simulant. Native pedal mucus, however, is still better than the best simulant; it provides comparable yield stress and restructuring time, but a lower post-yield viscosity.

A more general scientific question related to this work is how to characterize soft condensed matter under relevant loading conditions. One aspect of relevant characterization is the length scale of interest. It is noteworthy that no rheological measurements have been reported for native pedal mucus at the physiologically relevant gap thickness $h = 10 - 20\ \mu$m, including the results presented here. Most tests are reported with a gap height one to two orders of magnitude larger than this, and it is possible that native pedal mucus acts differently in a confined space. Effects of narrow gap polymer rheology such as gap-dependent relaxation times have been the subject of debate,[44] and gap-dependent yield stress levels as well as wall slip velocities have been observed with emulsions[45] and other complex fluids.[46]

The type of rheological test performed must also be relevant to the intended use of the material. Linear viscoelasticity is robust (in the linear regime), but may not fully apply to the intended use of the material. In this work, nonlinear rheological tests were used to quantify properties such as the yield stress, yield strain, and thixotropic restructuring time, as well as to investigate the nature of the yield transition and the existence of strain-stiffening in native slime. However, this strain-

stiffening could not be observed with the common measures of nonlinear viscoelasticity (G_1' and G_1''). This is in contrast to the colloidal gels examined by Gisler et al.[47] and the semi-flexible biopolymer gels studied by Storm et al.[10] in which strain-stiffening of the networks could be detected in the first harmonic elastic modulus, G_1'. This difference arises presumably from the differing flexibility of semi-flexible chains such as F-actin and the heavily glycosylated mucin protein studied here. In the present study, strain-stiffening can only be revealed by representing the raw data in the form of Lissajous curves. A suitable measure to quantify this local strain-stiffening behaviour has been derived[36] and will be the subject of a future publication.

Other ways also exist to characterize nonlinear rheology, such as the quantitative measures of nonlinearity suggested by Tee and Dealy[48], or the differential modulus devised by Gardel et al.[49] to describe actin networks. The differential modulus is measured while subjecting the material to a constant prestress, and is therefore readily used with elastically dominated systems, but may be less robust for softer, more lossy materials which are dominated by flow at large strains. In general, when soft condensed matter is exposed to large stresses or strains *in situ*, the nonlinear material properties will be significant, and one must decide which tests and measures provide the most relevant rheological fingerprint of the material.

Table 1 Summary of rheological properties of two simulants with similar apparent yield stresses compared with native gastropod pedal mucus. Although the concentrations and microscopic structure are different, fluids with similar yield stresses are compared since the macroscopic rheological property of a yield stress is the primary requirement for inclined adhesive locomotion, (Eq (1)).

	Native pedal mucus	Carbomer-based simulant (polymer gel)	Clay-based simulant (particulate gel)
Yield stress	100 - 240 Pa	108 Pa	90.8 Pa
Post-yield viscosity, η ($\dot{\gamma} = 10$ s^{-1})	10.4 - 25 Pa.s	31.6 Pa.s	9.6 Pa.s
G' ($\omega = 1$ rad.s^{-1})	200 Pa	540 Pa	1800 Pa
G' ($\omega = 1$ rad.s^{-1})	20 Pa	30 Pa	60 Pa
Yield stress transition	Sharp	Soft	Sharp
Pre-yield stiffening	Yes	No	No
Single exponential restructuring time, λ	0.85 s [adapted[43]]	0.8 s	17 s

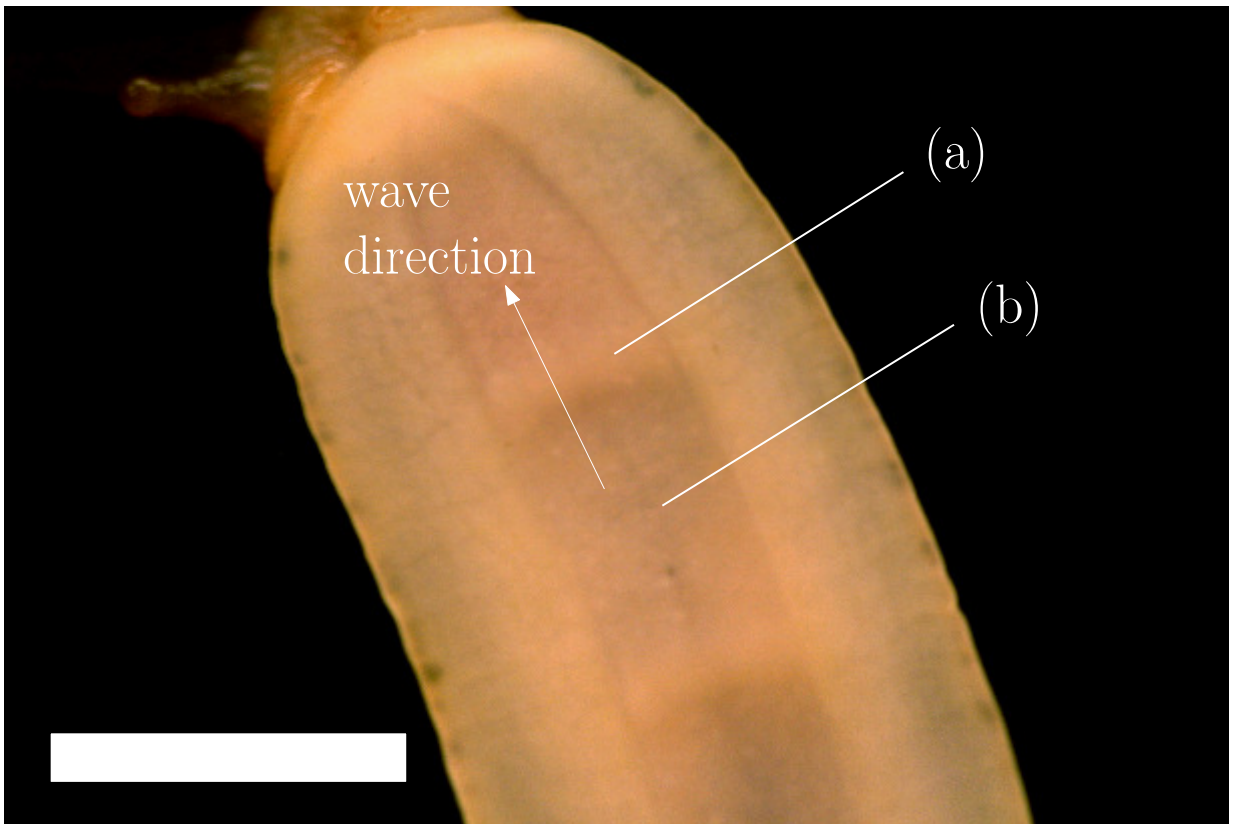

Figure 1 Bottom view of a crawling terrestrial slug Limax maximus, 1 cm scale bar; a) muscular contractions compress the foot parallel to the substrate, creating an area of high shear stress which ruptures the mucus network structure; b) an interwave of low stress allows the network structure to reform into a solid-like material which holds the organism to the substrate. Compression waves move toward the head (top of picture) during locomotion.

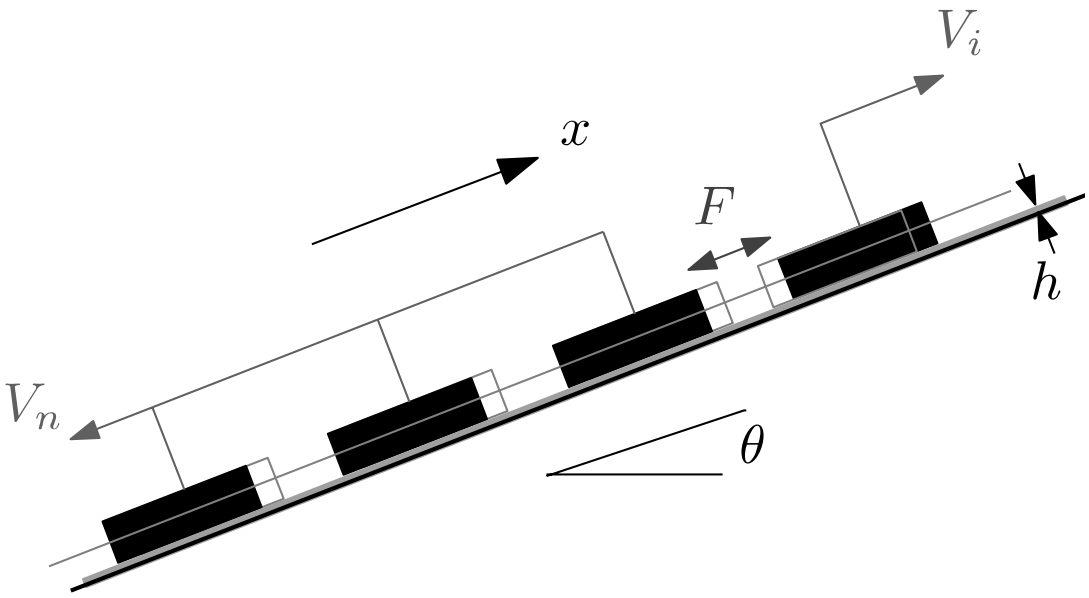

Figure 2 Simple model of an adhesive locomotion system – the crawler consists of *N* discrete pads and rests on a fluid with thickness *h*. An internal controlled force iteratively moves one pad forward with respect to the rest.

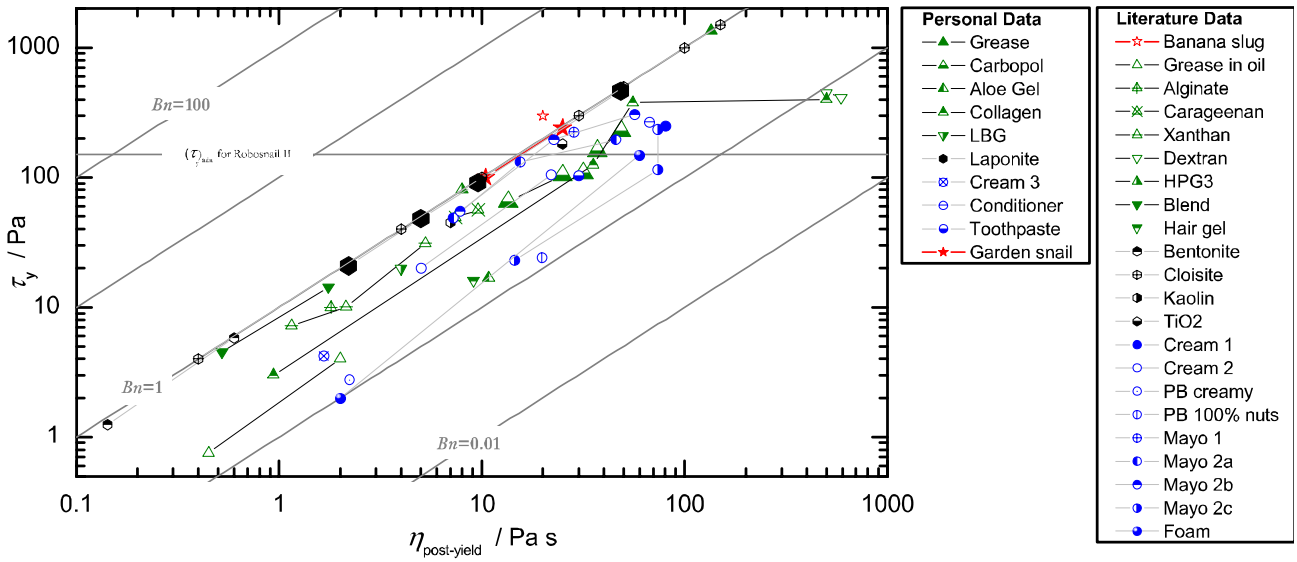

480 Figure 3 Material selection space comparing yield stress fluids; Stars: native mucus gels, Triangles: polymeric solutions and gels, Hexagons: Particulate suspensions and gels, Circles: soft glassy materials. A suitable simulant will meet a minimum yield stress requirement and have a low post-yield viscosity. See Electronic Supplemental Information (ESI) for material preparation and reference details.

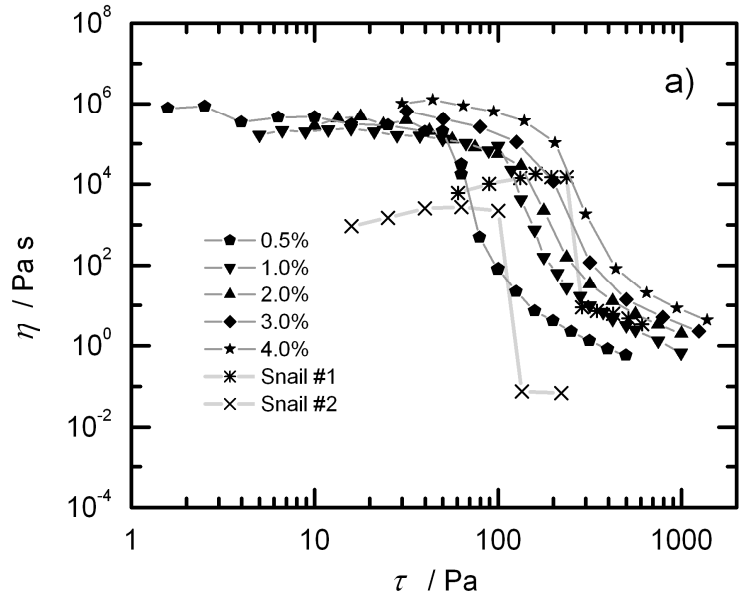

485

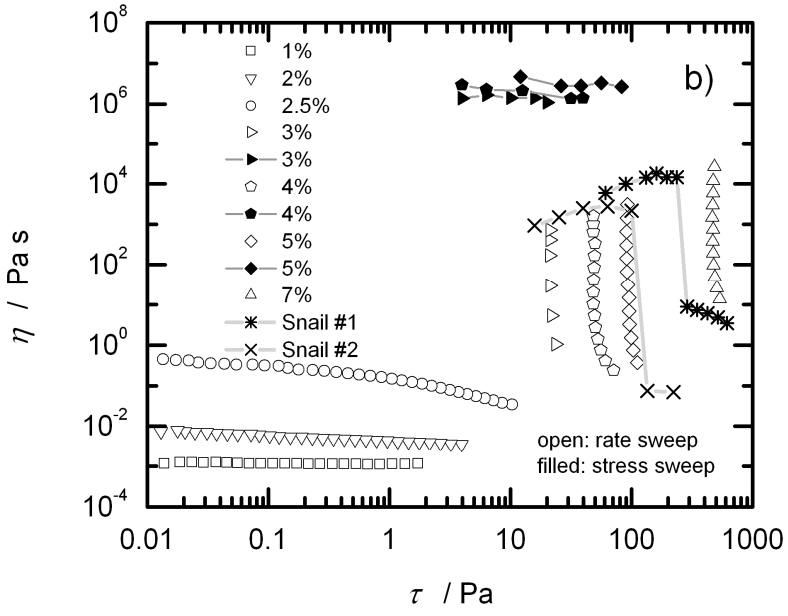

Figure 4 Steady shear viscosity of simulants compared to native pedal mucus from Helix aspera; native slime collected from two snails, tested with plate-plate fixtures D=0.8 mm with sandpaper, h=100 μm; a) Carbopol-based simulant, plate-plate with sandpaper, solvent trap, h=1000 μm, D=4 cm for 0.5%-2%, D=2 cm for 3%-4%; b) Laponite-based simulant, solvent trap, D=6 cm 1° cone-plate for 1%-2%, D=4 cm 2° cone-plate for 2.5%, D=4 cm plate-plate, h=1000 μm with sandpaper for 3%-7%.

490

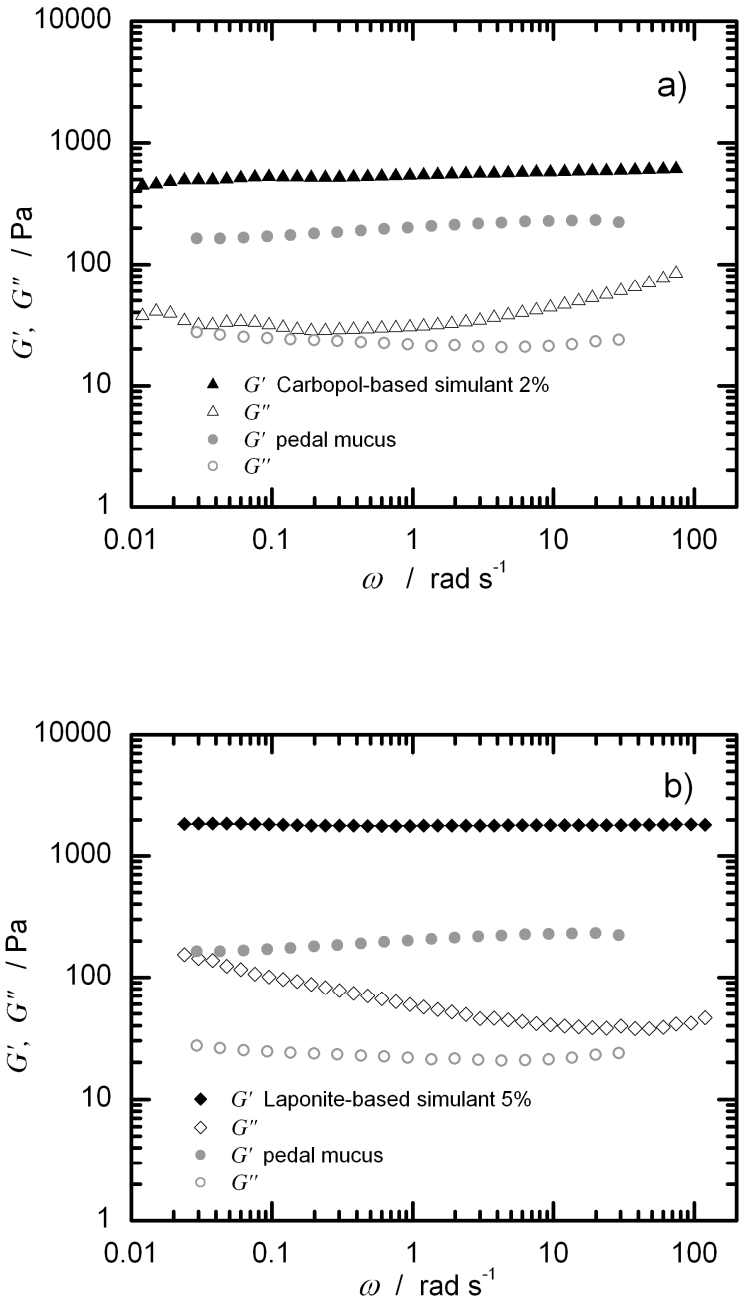

Figure 5 Linear viscoelastic moduli of simulants compared with native pedal mucus from Limax maximus; pedal mucus tested with D=2 cm plate with sandpaper, solvent trap, h=200 μm, τ0=5 Pa; simulants tested with D=4 cm plate with sandpaper, h=1000 μm, solvent trap; a) Carbopol-based simulant, , τ0=5 Pa; b) Laponite-based simulant, τ0=20 Pa

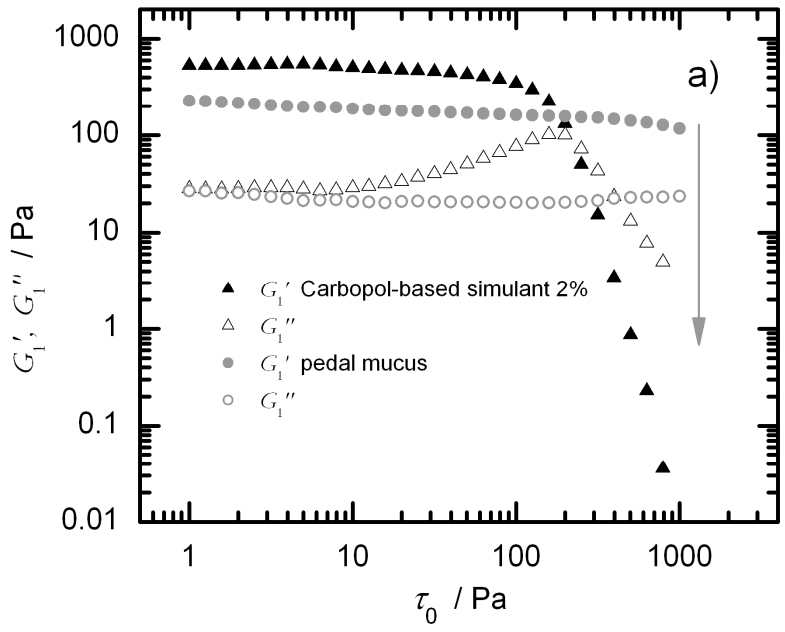

500

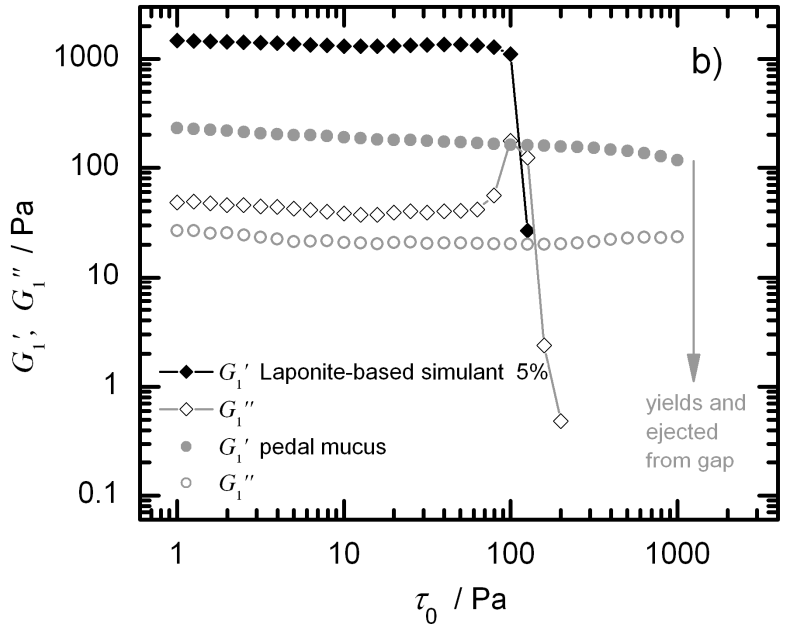

Figure 6 Large amplitude oscillatory shear (LAOS) of simulants compared with native pedal mucus from Limax maximus, same geometries as Figure 5, all samples tested at ω=1 rad.s^{-1}; a) Carbopol-based simulant; b) Laponite-based simulant.

505

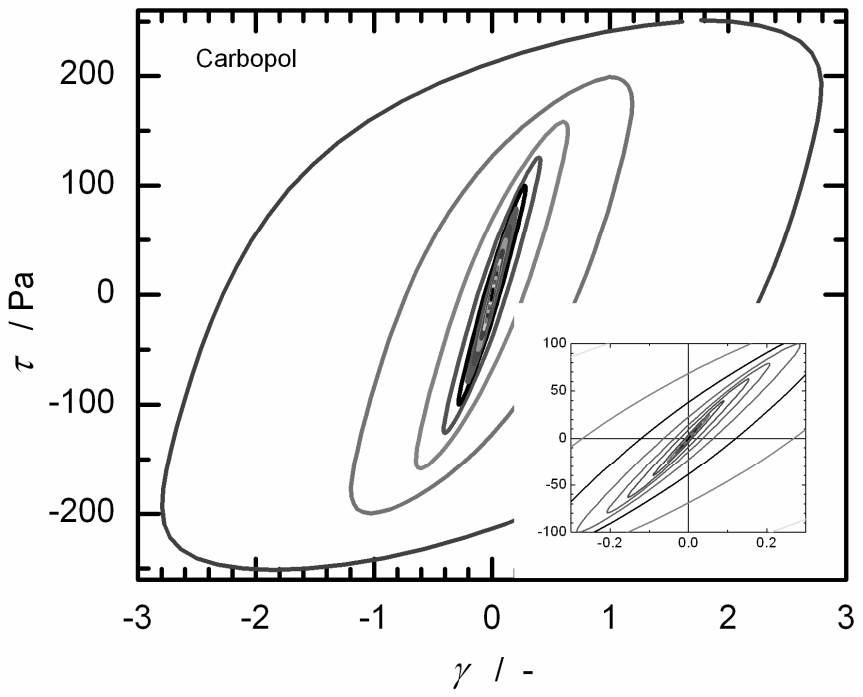

Figure 7 Lissajous curves resulting from the large amplitude oscillatory shear tests shown in Figure 6a for the polymer gel simulant.

510

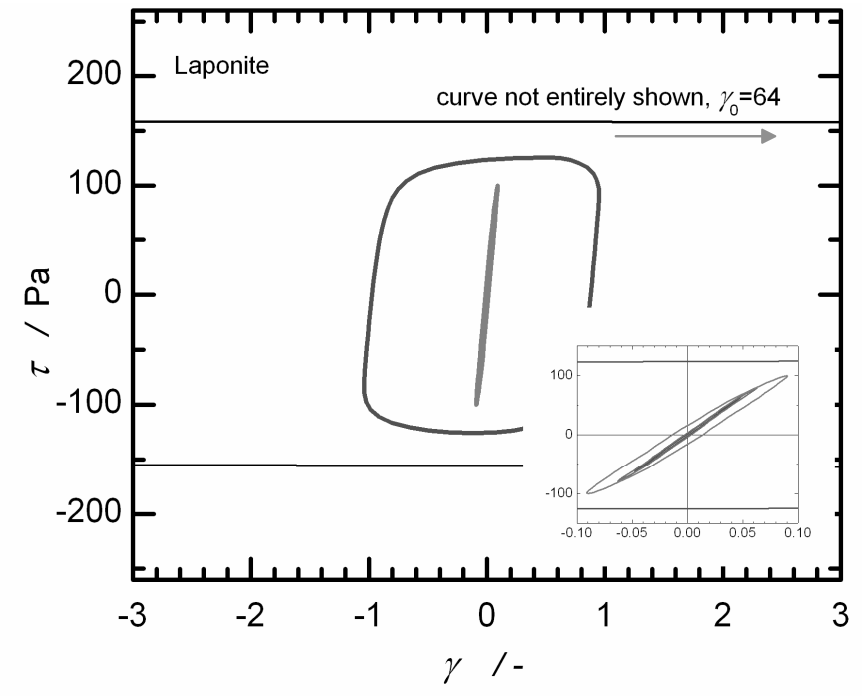

Figure 8 Lissajous curves resulting from the large amplitude oscillatory shear tests shown in Figure 6b for the particulate gel simulant.

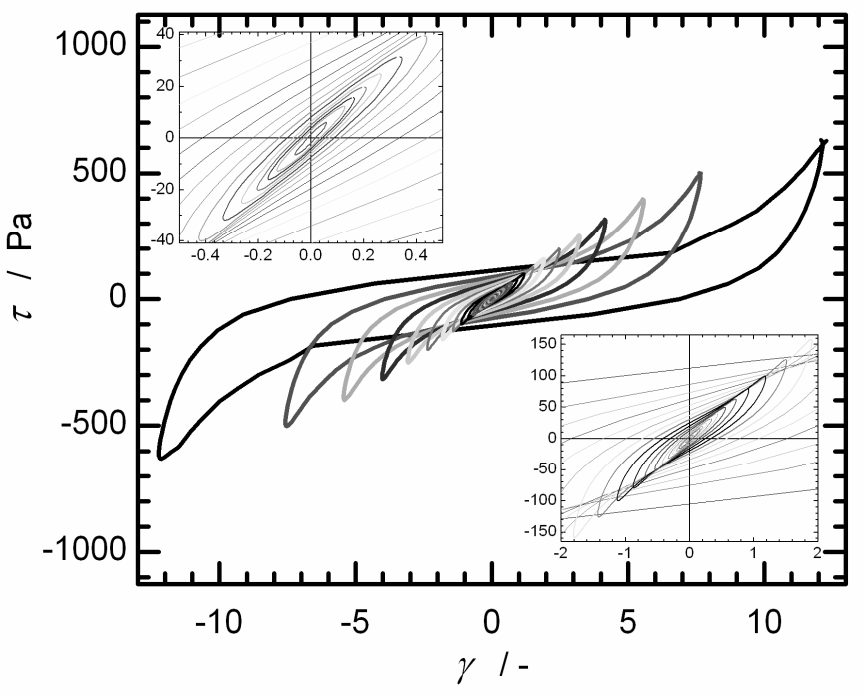

Figure 9 Lissajous curves resulting from the large amplitude oscillatory shear tests shown in Figure 6 for native pedal mucus from Limax maximus.

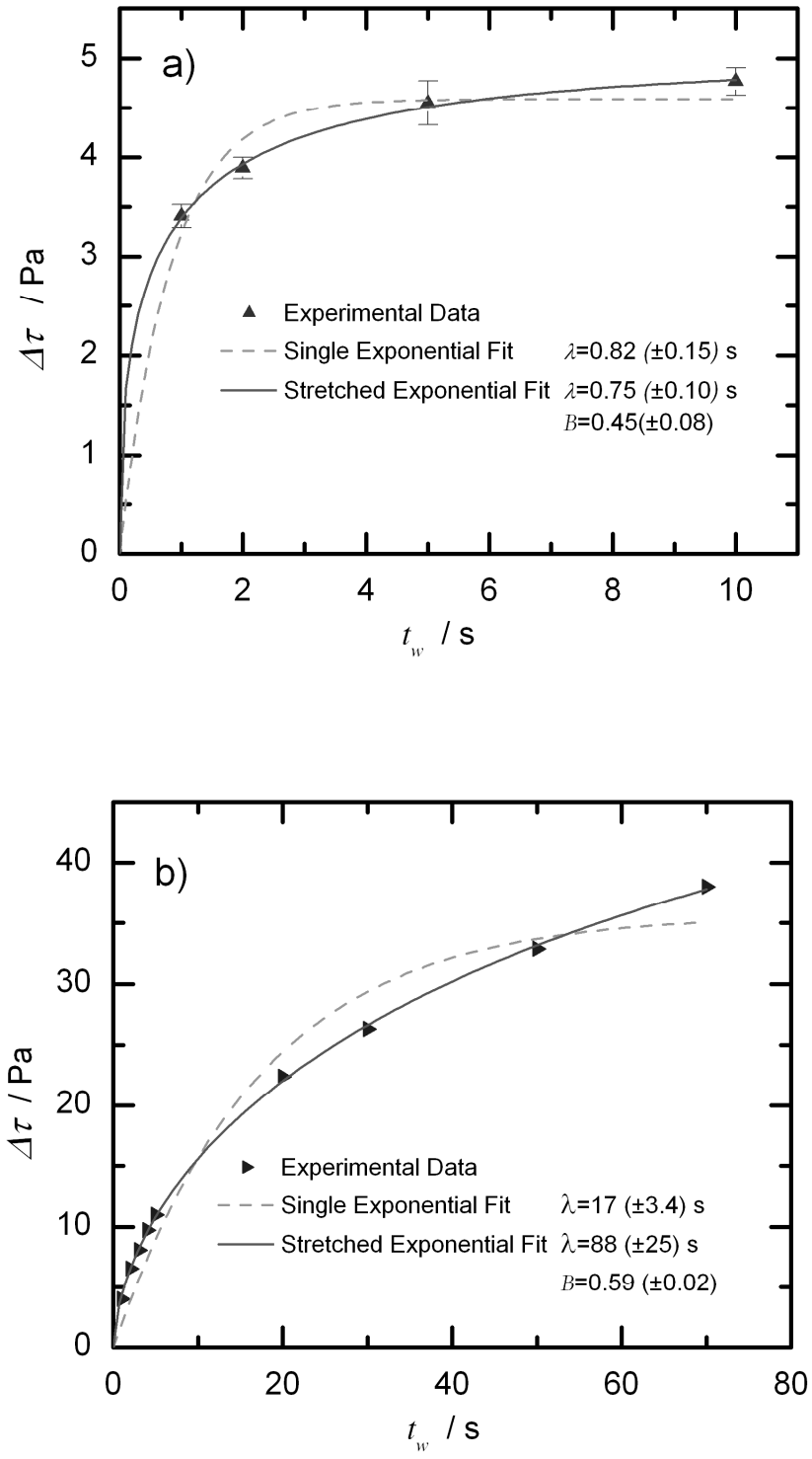

Figure 10 Time-dependent stress overshoot of simulants, D=5 cm 1° cone-plate; a) Carbopol 2%, error bars shown at one standard deviation; b) Laponite 3%

530

1. M. W. Denny, *Nature*, 1980, **285**, 160-161.
2. M. W. Denny and J. M. Gosline, *J. Exp. Biol.*, 1980, **88**, 375-393.
3. M. W. Denny, in *The Molluska*, ed. P. W. Hochachka, 1983, vol. 1. Metabolic Biochemistry and Molecular Biomechanics, pp. 431-465.
4. B. Chan, N. J. Balmforth and A. E. Hosoi, *Phys. Fluids A*, 2005, **17**, 113101.
5. J. O. Carnali and M. S. Naser, *Colloid Polym. Sci.*, 1992, **270**, 183-193.
6. N. W. Taylor and E. B. Bagley, *J. Appl. Polym. Sci.*, 1974, **18**, 2747-2761.
7. A. Mourchid, A. Delville, J. Lambard, E. Lecolier and P. Levitz, *Langmuir*, 1995, **11**, 1942-1950.
8. F. Pignon, A. Magnin, J. M. Piau, B. Cabane, P. Lindner and O. Diat, *Phys. Rev. E*, 1997, **56**, 3281-3289.
9. D. Bonn, H. Kellay, H. Tanaka, G. Wegdam and J. Meunier, *Langmuir*, 1999, **15**, 7534-7536.
10. C. Storm, J. J. Pastore, F. C. MacKintosh, T. C. Lubensky and P. A. Janmey, *Nature*, 2005, **435**, 191-194.
11. A. M. Smith and M. C. Morin, *Biol. Bull.*, 2002, **203**, 338-346.
12. Noveon, in *TDS 237*, http://www.personalcare.noveon.com/techdata/Carbopol980.asp, 1998.
13. A. Mourchid, E. Lecolier, H. Van Damme and P. Levitz, *Langmuir*, 1998, **14**, 4718-4723.
14. R. H. Ewoldt, M.S. Thesis, Dept. of Mechanical Engineering, Massachusetts Institute of Technology, 2006.
15. E. Carretti, L. Dei and R. G. Weiss, *Soft Matter*, 2005, **1**, 17-22.
16. S. B. Ross-Murphy, *J. Rheol.*, 1995, **39**, 1451-1463.
17. B. Chan, M.S. Thesis, Dept. of Mechanical Engineering, Massachusetts Institute of Technology, 2004.
18. H. A. Barnes, *J. Non-Newtonian Fluid Mech.*, 1997, **70**, 1-33.
19. P. C. F. Moller, J. Mewis and D. Bonn, *Soft Matter*, 2006, **2**, 274-283.
20. M. Denny, *Science*, 1980, **208**, 1288-1290.
21. E. Lauga and A. E. Hosoi, *Phys. Fluids A*, 2006, **18**, 113102.
22. R. Bird, R. Armstrong and O. Hassager, *Dynamics of Polymeric Liquids*, 2nd edn., John Wiley & Sons, Inc, New York, 1987.
23. M. W. Denny, *J. Exp. Biol.*, 1981, **91**, 195-217.
24. H. A. Barnes, *J. Non-Newtonian Fluid Mech.*, 1999, **81**, 133-178.
25. H. A. Barnes and K. Walters, *Rheol. Acta*, 1985, **24**, 323-326.
26. H. A. Barnes and D. Bell, *Korea-Aust. Rheol. J.*, 2003, **15**, 187-196.
27. H. A. Barnes, *J. Non-Newtonian Fluid Mech.*, 1995, **56**, 221-251.
28. D. M. Kalyon, P. Yaras, B. Aral and U. Yilmazer, *J. Rheol.*, 1993, **37**, 35-53.
29. A. Yoshimura and R. K. Prudhomme, *J. Rheol.*, 1988, **32**, 53-67.
30. R. G. Larson, *The structure and rheology of complex fluids*, Oxford University Press, New York, 1999. p.238
31. M. Wilhelm, *Macromol. Mater. Eng.*, 2002, **287**, 83-105.
32. K. Hyun, S. H. Kim, K. H. Ahn and S. J. Lee, *J. Non-Newtonian Fluid Mech.*, 2002, **107**, 51-65.
33. K. Miyazaki, H. M. Wyss, D. A. Weitz and D. R. Reichman, *Europhys. Lett.*, 2006, **75**, 915-921.
34. S. N. Ganeriwala and C. A. Rotz, *Polym. Eng. Sci.*, 1987, **27**, 165-178.
35. R. E. Shadwick, *Journal of Experimental Biology*, 1999, **202**, 3305-3313.
36. R. H. Ewoldt, A. E. Hosoi and G. H. McKinley, 78th Annual Meeting of The Society of Rheology, Portland, ME, Paper BS9, Oct. 9, 2006.
37. S. M. Fielding, P. Sollich and M. E. Cates, *J. Rheol.*, 2000, **44**, 323-369.
38. M. Cloitre, R. Borrega and L. Leibler, *Phys. Rev. Lett.*, 2000, **85**, 4819-4822.
39. R. Lapasin, L. DeLorenzi, S. Pricl and G. Torriano, *Carbohydr. Polym.*, 1995, **28**, 195-202.
40. A. H. Krall and D. A. Weitz, *Phys. Rev. Lett.*, 1998, **80**, 778-781.
41. J. R. Macdonald and J. C. Phillips, *J. Chem. Phys.*, 2005, **122**, 074510.
42. L. Heymann, E. Noack, L. Kaempfe and B. Beckmann, Proceedings of the XXIIth International Congress on Rheology, Laval University, Quebec City (Quebec), Canada, August 18-23, 1996.
43. M. W. Denny, *American Zoologist*, 1984, **24**, 23-36.
44. G. B. McKenna, *European Physical Journal E*, 2006, **19**, 101-108.
45. C. Clasen, B. P. Gearing and G. H. McKinley, *J. Rheol.*, 2006, **50**, 883-905.
46. C. Clasen and G. H. McKinley, *J. Non-Newton. Fluid Mech.*, 2004, **124**, 1-10.
47. T. Gisler, R. Ball and D. A. Weitz, *Phys. Rev. Lett.*, 1999, **82**, 1064-1067.
48. T. T. Tee and J. M. Dealy, *Transactions of the Society of Rheology*, 1975, **19**, 595-615.
49. M. L. Gardel, J. H. Shin, F. C. MacKintosh, L. Mahadevan, P. Matsudaira and D. A. Weitz, *Science*, 2004, **304**, 1301-1305.